

## Hydration-Induced Local Molecular Structures in Nano-Layered Clay Particles

K. Sato\*, K. Numata

Department of Environmental Sciences, Tokyo Gakugei University, Koganei, 184-8501 Tokyo, Japan

(Received 06 September 2012; published online 28 March 2013)

Positronium (Ps) annihilation spectroscopy and thermogravimetry and differential thermal analysis (TG-DTA) were conducted for synthetic smectite clay minerals to investigate local molecular structures induced by water adsorption and desorption. The TG curves indicate the weight loss of  $\sim 3.5$  wt %,  $\sim 2.5$  wt %, and  $\sim 2.0$  wt % for saponite, hectorite, and stevensite due to dehydration, in accordance with DTA endothermic peaks around 332 K, 350 K, and 345 K. It is found based on the results of Ps lifetime spectroscopy that the presence of angstrom-scale open space is sensitively dependent on water adsorption and desorption in smectite clay minerals.

**Keywords:** Smectite, Clay mineral, Positronium.

PACS numbers: 78.70.Bj, 68.43. – h

### 1. INTRODUCTION

Inorganic layered compounds known as clay minerals are of widespread importance for environmental materials as, e.g. functional catalyst, gas sensor, adsorption and separation technology, and so on [1]. In addition, they are increasingly of importance for dealing with the global environmental issues as, e.g., soil functionality [2] and giant earthquake nucleation [3]. Characteristic properties of clay minerals have been believed to be mostly correlated with hydration and dehydration occurring at the interlayer with typical spacing of a few nanometers. X-ray diffraction (XRD) [4], infrared spectroscopy [5], neutron diffraction and scattering [6], and nuclear magnetic resonance (NMR) spectroscopy [7], combined with thermal analysis (TG-DTA/DSC) have been extensively employed for investigating hydration and dehydration properties. It is now widely accepted that interlayer cations plays an essential role in understanding the hydration mechanism. In the present study, the local molecular structures induced by water adsorption and desorption are investigated for three kinds of smectite clay minerals by positronium (Ps), positron-electron bound state like hydrogen atom.

### 2. EXPERIMENTAL PROCEDURE

The following synthetic smectite clay minerals provided by Kunimine Industries Co. Ltd., Japan were examined in this study: Na-type saponite (54.71 %  $\text{SO}_2$ , 5.02 %  $\text{Al}_2\text{O}_3$ , 0.03 %  $\text{Fe}_2\text{O}_3$ , 30.74 %  $\text{MgO}$ , 2.15 %  $\text{Na}_2\text{O}$ , 0.07 %  $\text{CaO}$ , 0.67 %  $\text{SO}_3$ , 6.64 %  $\text{H}_2\text{O}$ ), Na-type hectorite (56.41 %  $\text{SO}_2$ , 0.04 %  $\text{Al}_2\text{O}_3$ , 27.50 %  $\text{MgO}$ , 1.12 %  $\text{Li}_2\text{O}$ , 6.32 %  $\text{Na}_2\text{O}$ , 0.14 %  $\text{CaO}$ , 1.10 %  $\text{SO}_3$ , 7.35 %  $\text{H}_2\text{O}$ ), and Na-type stevensite (56.70 %  $\text{SO}_2$ , 0.05 %  $\text{Al}_2\text{O}_3$ , 27.51 %  $\text{MgO}$ , 6.90 %  $\text{Na}_2\text{O}$ , 0.13 %  $\text{CaO}$ , 1.18 %  $\text{SO}_3$ , 7.48 %  $\text{H}_2\text{O}$ ). The particle size is approximately 45 nm in diameter.

Dehydration behavior was investigated by thermogravimetry and differential thermal analysis (TG-DTA

2020SA, BRUKER AXS Co. Ltd.) at a heating rate of  $5 \text{ K} \cdot \text{min}^{-1}$  under  $\text{N}_2$  atmosphere with  $\alpha$ -alumina ( $\alpha$ - $\text{Al}_2\text{O}_3$ ) standard material.

The sizes of open spaces and their fractions were investigated by positronium (Ps) annihilation lifetime spectroscopy [8-10]. A fraction of energetic positrons injected into samples forms the bound state with an electron, Ps. Singlet *para*-Ps (*p*-Ps) with the spins of the positron and electron antiparallel and triplet *ortho*-Ps (*o*-Ps) with parallel spins are formed at a ratio of 1 : 3. Hence, three states of positrons: *p*-Ps, *o*-Ps, and free positrons exist in samples. The annihilation of *p*-Ps results in the emission of two  $\gamma$ -ray photons of 511 keV with lifetime  $\sim 125$  ps. Free positrons are trapped by negatively-charged parts such as polar elements and annihilated into two photons with the lifetime  $\sim 450$  ps. The positron in *o*-Ps undergoes two-photon annihilation with one of the bound electrons with a lifetime of a few ns after localization in angstrom-scale pores. The last process is known as *o*-Ps pick off annihilation and provides information on the free volume size  $R$  through its lifetime  $\tau_{o\text{-Ps}}$  based on the Tao-Eldrup model: [11-12]

$$\tau_{o\text{-Ps}} = 0.5 \left[ 1 - \frac{R}{R_0} + \frac{1}{2\pi} \sin \left( \frac{2\pi R}{R_0} \right) \right]^{-1}, \quad (2.1)$$

where  $R_0 = R + \Delta R$ , and  $\Delta R = 0.166$  nm is the thickness of homogeneous electron layer in which the positron in *o*-Ps annihilates. The positron source ( $^{22}\text{Na}$ ), sealed in a thin foil of Kapton, was mounted in a sample-source-sample sandwich. The validity of our lifetime measurements in addition to the data analysis was confirmed with certified reference materials (NMIJ CRM 5601-a and 5602-a) provided by National Metrology Institute of Japan, National Institute of Advanced Industrial Science and Technology (AIST) [13-14]. Positron lifetime spectra were numerically analyzed using the POSITRONFIT code [15].

\* sato-k@u-gakugei.ac.jp

The article was reported at the 2<sup>nd</sup> International Conference «Nanomaterials: Applications & Properties-2012»

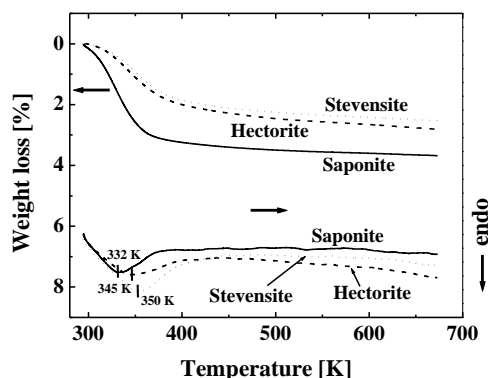


Fig. 1 – TG-DTA data for saponite (solid lines), hectorite (dashed lines), and stevensite (dotted lines)

### 3. RESULTS AND DISCUSSION

Fig. 1 shows TG-DTA data for the hydrated saponite, hectorite, and stevensite. The TG curve for the saponite begins to decrease drastically upon heating and continues to decrease up to 423 K with the weight loss of  $\sim 3.5$  wt %. This is due to desorption of water molecules from  $\text{Na}^+$  cations in interlayers, which coincides with an endothermic peak around 332 K in the DTA curve. The TG curves observed for hectorite and stevensite exhibit the weight loss of  $\sim 2.5$  wt % and  $\sim 2.0$  wt %, respectively, indicating dehydration behavior similar to that of the saponite. The endothermic peaks in the DTA curve for the hectorite and stevensite appears around 345 K and 350 K, respectively, which are significantly higher than for the saponite. The results indicate that water molecules more strongly adsorbed onto  $\text{Na}^+$  cations in the order of saponite, hectorite, and stevensite.

Fig. 2 shows positron lifetime spectra for the hydrated saponite (a), hectorite (b), and stevensite (c) as well as those of dehydrated samples. The significant changes owing to dehydration can be clearly seen in the lifetime spectra for three samples. The lifetime spectrum for the hydrated saponite was analyzed with respect to three components of lifetimes. On the other hand, four-component analysis was performed for the dehydrated saponite. The lifetime spectra for both the samples of the hydrated and dehydrated hectorite were analyzed with respect to four components of lifetimes. Four-component analyses were successfully conducted for both the samples of the hydrated and dehydrated stevensite as well. The longest-lived component  $\tau_4$  and second longest-lived component  $\tau_3$  are attributable to pick-off annihilation of *o*-Ps associated with angstrom-scale open spaces in smectite clay minerals.

Table 1 lists evaluated lifetimes of *o*-Ps pick-off annihilation  $\tau_3$  and  $\tau_4$  and corresponding open space sizes  $R_3$  and  $R_4$  together with their relative intensities ( $I_3$  and  $I_4$ ) observed for three smectite samples. The lifetime  $\tau_3$  of  $\sim 2$  ns was observed for the hydrated saponite. After dehydrating at 423 K for 8 h in vacuum at  $\sim 10^{-5}$  Torr, a very long lifetime  $\tau_4$  of  $\sim 24$  ns appears with its fraction  $I_4 \sim 13$  %. The size of open space derived from lifetime  $\tau_3$  through Eq. (2.1) is  $\sim 3$  Å in radius, whereas the size derived from lifetime  $\tau_4$  is

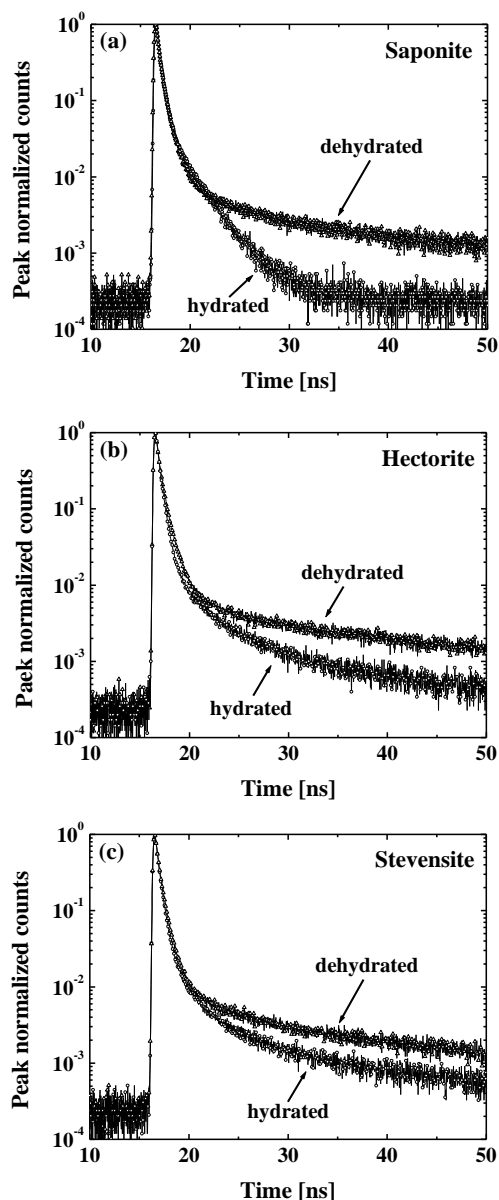


Fig. 2 – Positron lifetime spectra for saponite (a), hectorite (b), and stevensite (c). The data for both the hydrated and dehydrated samples are presented

$\sim 10$  Å. For the hydrated hectorite, the lifetimes of *o*-Ps pick-off annihilation  $\tau_3$  ( $\sim 3$  ns) and  $\tau_4$  ( $\sim 15$  ns) corresponding to the open spaces with the sizes of  $\sim 4$  Å and  $\sim 8$  Å are evaluated with their relative intensities  $I_3$  ( $\sim 14$  %) and  $I_4$  ( $\sim 5$  %). After dehydrating, the lifetime  $\tau_4$  and its intensity  $I_4$  increase up to  $\sim 25$  ns and  $\sim 15$  %, respectively. This indicates that the size of open space increases together with its fraction. The lifetimes of *o*-Ps pick-off annihilation  $\tau_3$  ( $\sim 3$  ns) and  $\tau_4$  ( $\sim 16$  ns) corresponding to the open spaces with the sizes of  $\sim 3$  Å and  $\sim 8$  Å are observed for the hydrated stevensite with their relative intensities  $I_3$  ( $\sim 9$  %) and  $I_4$  ( $\sim 6$  %). Similarly to the hectorite, dehydration at 423 K for 8 h in vacuum increases the lifetime  $\tau_4$  and intensity  $I_4$  up to  $\sim 26$  ns and 14 %, respectively.

It is of great interest that Ps annihilation spectroscopy reveals the angstrom-scale open spaces susceptible

**Table 1** – *o*-Ps pick-off lifetimes  $\tau_3$  and  $\tau_4$  and corresponding open space sizes  $R_3$  and  $R_4$  together with their fractions  $I_3$  and  $I_4$  observed for three smectite samples

	$\tau_3$ [ns]	$I_3$ [%]	$\tau_4$ [ns]	$I_4$ [%]	$R_3$ [Å]	$R_4$ [Å]
Saponite						
hydrated	2.2	21	–	–	3.0	–
dehydrated	3.1	6	23.9	13	3.7	9.5
Hectorite						
hydrated	2.8	14	14.5	5	3.5	7.6
dehydrated	2.6	6	25.1	15	3.4	9.7
Stevensite						
hydrated	2.6	9	16.3	6	3.4	8.1
dehydrated	3.7	6	26.2	14	4.1	9.8

to water adsorption and desorption for three smectite samples. The size of smaller open space  $R_3$  shows insignificant changes regardless of water adsorption and desorption (see Table 1). The interlayer spaces for the dehydrated smectite completely shrink  $\text{Na}^+$  cations infilling up the hexagonal cavity of silicate tetrahedron, as confirmed by XRD experiments [16]. Generally, they expand together with water molecules adsorbed onto the  $\text{Na}^+$  cations in the interlayer spaces due to hydration. It is thus unlikely that the smaller open space without significant change of open space size (3 Å ~ 4 Å) corresponds to the interlayer space.

The larger open space with its size  $R_4$  ranging from ~ 7 Å to ~ 10 Å is in turn too large to relate with the interlayer space. It is thus inferred the presence of angstrom-scale open spaces that have been unconsidered for the molecular model of inorganic layered materials so far.

#### 4. CONCLUSIONS

Three kinds of smectite clay minerals, saponite, hectorite, and stevensite were investigated by positronium (Ps) annihilation spectroscopy and thermogravimetry and differential thermal analysis (TG-DTA). Based on the results of TG-DTA, hydration is found to occur easier in the order of saponite, hectorite, and stevensite. Ps lifetime spectroscopy reveals that the presence of angstrom-scale open space is sensitively dependent on hydration / dehydration state of smectite clay minerals.

#### ACKNOWLEDGEMENTS

Discussion with K. Fujimoto (Tokyo Gakugei University) and K. Kawamura (Okayama University) is gratefully appreciated. This work was partially supported by a Grant-in-Aid of the Japanese Ministry of Education, Science, Sports and Culture (Grant Nos. 21540317 and 23740234).

#### REFERENCES

1. K. Selvam, M. Swaminathan, *Chem. Lett.* **36**, 1060 (2007).
2. I.M. Young, J.W. Crawford, *Science* **304**, 1634 (2004).
3. C.A.J. Wibberley, T. Shimamoto, *Nature* **436**, 689 (2005).
4. J.M. Cases, I. Bérend, M. Francois, J.P. Uriot, L.J. Michot, F. Thomas, *Clay. Clay Miner.* **45**, 8 (1997).
5. J.L. Bishop, C.M. Pieters, J.O. Edwards, *Clay. Clay Miner.* **42**, 702 (1994).
6. C. Poinson, *Solid State Ionics* **97**, 399 (1997).
7. A. Delville, M. Letellier, *Langmuir* **11**, 1361 (1995).
8. K. Sato, H. Murakami, K. Ito, K. Hirata, Y. Kobayashi, *Macromolecules* **42**, 4853 (2009).
9. K. Sato, K. Fujimoto, M. Nakata, T. Hatta, *J. Phys. Chem. C* **115**, 18131 (2011).
10. K. Sato, *J. Phys. Chem. B* **115**, 14874 (2011).
11. S.J. Tao, *J. Chem. Phys.* **56**, 5499 (1972).
12. M. Eldrup, D. Lightbody, J.N. Sherwood, *Chem. Phys.* **63**, 51 (1981).
13. K. Ito, T. Oka, Y. Kobayashi, Y. Shirai, H. Saito, Y. Honda, Y. Nagai, M. Fujinami, A. Uedono, K. Sato, T. Hirade, A. Shimazu, H. Hosomi, K. Sakaki, *J. Appl. Phys.* **104**, 0261021 (2008).
14. K. Ito, T. Oka, Y. Kobayashi, Y. Shirai, K. Wada, M. Matsumoto, M. Fujinami, T. Hirade, Y. Honda, H. Hosomi, Y. Nagai, K. Inoue, H. Saito, K. Sakaki, K. Sato, A. Shimazu, A. Uedono, *Mater. Sci. Forum* **607**, 248 (2009).
15. P. Kirkegaard, M. Eldrup, *Comput. Phys. Commun.* **7**, 401 (1974).
16. S. Morodome, K. Kawamura, *Clay. Clay. Miner.* **57**, 150 (2009).